JVI Journals.ASM.org

A Novel Cytotoxic Sequence Contributes to Influenza A Viral Protein PB1-F2 Pathogenicity and Predisposition to Secondary Bacterial Infection

Irina V. Alymova,[a,b] Amali Samarasinghe,[e] Peter Vogel,[c] Amanda M. Green,[b] Ricardo Weinlich,[d] Jonathan A. McCullers[b,e]

Influenza Division, National Center for Immunization & Respiratory Diseases, Centers for Disease Control & Prevention, Atlanta, Georgia, USA[a]; Departments of Infectious Diseases,[b] Pathology,[c] and Immunology,[d] St. Jude Children's Research Hospital, Memphis, Tennessee, USA; Department of Pediatrics, University of Tennessee Health Sciences Center, Memphis, Tennessee, USA[e]

Enhancement of cell death is a distinguishing feature of H1N1 influenza virus A/Puerto Rico/8/34 protein PB1-F2. Comparing the sequences (amino acids [aa] 61 to 87 using PB1-F2 amino acid numbering) of the PB1-F2-derived C-terminal peptides from influenza A viruses inducing high or low levels of cell death, we identified a unique I68, L69, and V70 motif in A/Puerto Rico/8/34 PB1-F2 responsible for promotion of the peptide's cytotoxicity and permeabilization of the mitochondrial membrane. When administered to mice, a 27-mer PB1-F2-derived C-terminal peptide with this amino acid motif caused significantly greater weight loss and pulmonary inflammation than the peptide without it (due to I68T, L69Q, and V70G mutations). Similar to the wild-type peptide, A/Puerto Rico/8/34 elicited significantly higher levels of macrophages, neutrophils, and cytokines in the bronchoalveolar lavage fluid of mice than its mutant counterpart 7 days after infection. Additionally, infection of mice with A/Puerto Rico/8/34 significantly enhanced the levels of morphologically transformed epithelial and immune mononuclear cells recruited in the airways compared with the mutant virus. In the mouse bacterial superinfection model, both peptide and virus with the I68, L69, and V70 sequence accelerated development of pneumococcal pneumonia, as reflected by increased levels of viral and bacterial lung titers and by greater mortality. Here we provide evidence suggesting that the newly identified cytotoxic sequence I68, L69, and V70 of A/Puerto Rico/8/34 PB1-F2 contributes to the pathogenesis of both primary viral and secondary bacterial infections.

Influenza A viruses (IAVs), members of the *Orthomyxoviridae* family with a segmented, negative-stranded RNA genome, are among the most common pathogens in humans and animals (1). IAVs have multiple features that contribute to their ability to cause pandemics and greatly enhance secondary bacterial infections (2). Since its discovery in 2001 (3), the IAV PB1-F2 protein has been viewed as an important factor in viral virulence because of its association with the pathogenicity of H1N1 1918, H2N2 1957, and H3N2 1968 pandemic viruses and highly pathogenic avian influenza viruses of the H5N1 subtype (4–7). In addition, the PB1-F2 proteins from H1N1 1918 and 1934 and H3N2 1968 viruses elevated mortality in mice due to the development of secondary bacterial infection as a result of increased bacterial lung titers and progression to generalized pneumonia (6–8).

Originally described as an 87-amino-acid (aa)-residue accessory protein of A/Puerto Rico/8/34 (H1N1; here referred to as PR8), the PB1-F2 is encoded in the +1 open reading frame (ORF) of the PB1 gene segment of most human and avian IAVs (9). The findings from numerous studies indicate that, depending on the IAV strain, PB1-F2 may elicit diverse effects such as death in infected cells (10–14), upregulation of viral polymerase activity (15–18), increased inflammation (19–22), and, as recently reported, direct antibacterial activity (8).

PB1-F2 can enhance cell death by a variety of mechanisms. The apoptotic properties of the PR8 PB1-F2 protein are linked to its predominant mitochondrial localization in infected and transfected cells (3, 10, 14). Mitochondrial localization of PB1-F2 is achieved by the mitochondrial targeting sequence, a short α-helical arginine-rich motif at the C terminus of the protein, spanning aa 65 to 87 (10, 14, 23). PB1-F2 initiates the intrinsic pathway of apoptosis through permeabilization of the mitochondrial membranes (6, 11–14), resulting in the loss of respiratory function, release of intermembrane proteins (such as cytochrome *c*) into the cytosol, activation of caspase-9 and caspase-3, and cell death. The exact mechanism of PB1-F2-mediated mitochondrial outer membrane permeabilization (MOMP) is not clear. Early studies suggested a direct primary interaction of PB1-F2 with two proteins involved in the formation of the mitochondrial permeability transition pore complex, ANT3 and VDAC1, for apoptotic stimuli (14). Later work proposed the initial activation of the cellular proapoptotic BAX/BAK proteins from the Bcl-2 family for interaction with the outer mitochondrial membrane, stimulation of the VDAC1 opening, and apoptosis induction (6). Another (not related to MOMP) mechanism of PB1-F2-mediated cell death was recently reported (24). Influenza A virus PB1-F2 protein was shown to adopt a β-sheet secondary structure, forming amyloid fibers and β-amyloid pore structures and leading to permeabilization of cellular membranes and eventually to cell death.

A recent study by us showed that PB1-F2-mediated cell death is virus strain specific (6). Thus, among tested 27-mer (aa 61 to 87) peptides derived from PB1-F2 C-terminal sequences of PR8, pandemic strains 1918, 1957, and 1968 (a recent highly pathogenic

Received 22 May 2013 **Accepted** 3 October 2013
Published ahead of print 30 October 2013
Address correspondence to Irina V. Alymova, ialymova@cdc.gov.

doi:10.1128/JVI.01373-13

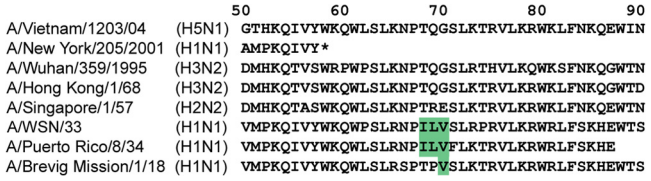

FIG 1 Amino acid sequences of influenza A virus PB1-F2 proteins. Sequences are shown for selected influenza A virus strains. Green shading highlights amino acids that we propose are a cause of a high level of cell death due to the A/Puerto Rico/8/1934 (H1N1) PB1-F2 protein.

avian IAV of the H5N1 subtype), and the recent 1995 seasonal H3N2 strain, only the PR8 PB1-F2-derived peptide was able to induce MOMP and a high level of cell death. Similar to the PB1-F2-derived peptide, the PR8 virus induced the most death in cell cultures in that study. Analysis of C-terminal PB1-F2 sequences (aa 61 to 87) from viruses used in that study (Fig. 1) revealed four amino acid residues, Ile 68 (I68), Leu 69 (L69), Val 70 (V70), and Phe 71 (F71), uniquely present within the C-terminal end of PR8 PB1-F2, suggesting the possibility of their involvement in the virus cell death phenotype. The only exception was the H1N1 1918 virus, which also had V70 residues on its PB1-F2 (Fig. 1). Interestingly, the H1N1 1918 was second to PR8 in showing an enhanced cell death phenotype in our previously published work (6). We further examined whether another influenza virus, A/William Smith Neurotropic/33 (H1N1; here referred to as WSN), whose PB1-F2 protein was shown to be associated with cell death responses (20, 21), had these identified amino acid residues. We found that the C-terminal end of the WSN PB1-F2 protein had three (I68, L69, and V70) amino acid residues of interest (Fig. 1). The Phe of PR8 was replaced by Ser at residue 71 on WSN PB1-F2, suggesting the possibility for three amino acid residues of PB1-F2, I68, L69, and V70, to be a minimal requirement for cell death enhancement.

To test this hypothesis, we generated a PR8 PB1-F2 C-terminal peptide and a virus variant with mutations designed to knock out the proposed cell death sequence. Comparing the properties of two distinct peptides, we found that the trio of amino acids I68, L69, and V70 promotes death in exposed cell cultures. This sequence supports PR8 virulence and enhances lung inflammation and predisposition to secondary bacterial infection in mice. Our findings provide new insights into the pathogenicity of the IAV PB1-F2 protein and highlight the role of this protein in promoting secondary bacterial infections.

MATERIALS AND METHODS

Peptides. Using the predicted amino acid sequences of C-terminal parts (aa 61 to 87) of PB1-F2 proteins from viruses inducing high (PR8 and WSN) and low (pandemic strains H1N1 1918, H2N2 1957, and H3N2 1968; highly pathogenic avian influenza viruses of the H5N1 subtype; and the recent 1995 seasonal H3N2 strain) levels of death (Fig. 1), the 27-mer peptides from the PR8 and H3N2 A/Wuhan/359/1995 (Wuh95) C-terminal ends with no, single, or multiple substitutions at positions 68, 69, and 70 (using PB1-F2 amino acid numbering) were synthesized by GenScript Corp. (Piscataway, NJ). Mutations (Ile 68 to Thr [I68T], Leu 69 to Gln [L69Q], and Val 70 to Gly [V70G]) to the PR8 C-terminal peptide (PR8/C) were made to emulate the amino acid residues present in the Wuh95 PB1-F2 peptide (Wuh95/C), which does not cause cell death (6) or pathogenicity (8) in mice. The PR8 PB1-F2 peptide with the three key mutations, I68T, L69Q, and V70G, was designated PR8/C-3. Similarly, a mutant peptide on a Wuh95 background was made with three reciprocal substitutions (Thr 68 to Ile [T68I], Gln 69 to Leu [Q69L], and Gly 70 to Val [G70V]). The Wuh95 PB1-F2 peptide with these inverse mutations was designated Wuh95/C + 3. Before use in *in vitro* and *in vivo* experiments, peptides provided as a lyophilized powder were initially solubilized in phosphate-buffered saline (PBS) (pH 5.0) and subsequently diluted in PBS (pH 7.2) to adjust the pH to 6.0 in a final solution.

Cell cultures. Madin-Darby canine kidney (MDCK) and A549 human alveolar adenocarcinoma epithelium cells were grown in 1× minimum essential medium that contained 5% fetal bovine serum (FBS). Human kidney 293T epithelium cells were maintained in Dulbecco's modified Eagle's medium supplemented with 10% FBS. U937 human leukemic monocyte lymphoma cells were grown in RPMI 1640 medium that contained 10% FBS. In cell infection assays, the FBS in the growth media was replaced by bovine serum albumin (BSA).

Infectious agents. PR8 and its mutant variant were generated by reverse genetics as previously described (25). Before rescue, the PB1 gene segment of PR8 was modified using site-directed mutagenesis (QuikChange; Stratagene, La Jolla, CA) by previously described methods (7) to generate a virus variant with I68T, L69Q, and V70G mutations in the PB1-F2 ORF (PR8-3) to knock out the sequence with proposed apoptotic activity. Inserted mutations in the PB1-F2 did not cause nonsynonymous changes in the PB1 reading frame. The rescued viruses were amplified once in MDCK cells for stocks, and the PB1 gene segments were fully sequenced to confirm that they were free of mutations other than those described. Infectivity of the rescued viruses was determined using plaque assays in MDCK cells, as described elsewhere (26).

Streptococcus pneumoniae (SPn) strain A66.1 (type 3) was grown in Todd-Hewitt broth (Difco Laboratories, Detroit, MI) to an optical density at 620 nm (OD_{620}) of approximately 0.4 and then frozen at −80°C mixed 2:1 with 5% sterile glycerol. The titers of the frozen stocks were quantitated on tryptic soy agar (Difco Laboratories, Detroit, MI) supplemented with 3% (vol/vol) sheep erythrocytes.

Mitochondrial outer membrane permeabilization assays. Heavy membrane fractions (mitochondria) were purified from fresh mouse (C57BL/6J strain) liver using Dounce homogenization and differential centrifugation in mitochondrial isolation buffer (200 mM mannitol, 68 mM sucrose, 10 mM HEPES-KOH [pH 7.4], 10 mM KCl, 1 mM EDTA, 1 mM EGTA, and 0.1% BSA). For MOMP assays, mitochondria were incubated in mitochondrial isolation buffer supplemented to 100 mM KCl (mitochondrial permeabilization assay buffer) with or without caspase-8-cleaved mouse BID (R&D Systems, Inc., Minneapolis, MN) or PR8 PB1-F2-derived peptides at various final concentrations ranging from 10 to 1,000 μM for 45 min at 37°C. Reaction mixtures were then fractionated into supernatants and pellets by centrifugation at 5,500 × *g* for 5 min and analyzed by SDS-PAGE and Western blot analysis with anti-cytochrome *c* antibodies (clone 7H8.2C12; BD Biosciences Pharmingen, San Diego, CA). Supernatant and pellet fractions were separated using Criterion XT 4% to 12% resolving gel (Bio-Rad, Hercules, CA) with 1× MES [2-(*N*-morpholino)ethanesulfonic acid] buffer at 150 V. Proteins were transferred to nitrocellulose by standard Western analysis conditions, blocked in 5% milk–Tris-buffered saline with Tween 20 (TBST), and incubated with the primary anti-cytochrome *c* antibody at 1:1,000 in blocking buffer overnight at 4°C. The secondary antibody (1:5,000 in blocking buffer) was incubated at room temperature (RT) for 1 h before standard enhanced chemiluminescence detection. For MOMP assays, all peptides were initially resuspended in anhydrous dimethyl sulfoxide (DMSO) (5 mM) and subsequently diluted in mitochondrial permeabilization assay buffer to a final concentration.

Cell culture assays. To assess the cytotoxicity of PB1-F2-derived peptides, a suspension of MDCK, A549, or U937 cells (2.0×10^6 per ml) in growth medium was exposed to 100 μM (final concentration) PR8 or Wuh95 peptides or PBS for 1 h. Next, the cell suspension was mixed with 0.4% trypan blue, and the numbers of dead (stained) and living (unstained) cells in the sample were determined by using a Countess auto-

dently and scored as follows: 1 = minimal, focal to multifocal, inconspicuous; 2 = mild, multifocal, conspicuous; 3 = moderate, multifocal, prominent; 4 = marked, multifocal coalescing, lobar; 5 = severe, extensive, diffuse, with consolidation, multilobar. The overall severity score for each lung was obtained by totaling all of the individual lesion scores, and average group scores were calculated from these totals. For immunohistochemical detection of podoplanin on the surface of type I pneumocytes, lung sections were mounted on positively charged glass slides (Superfrost Plus, Fisher Scientific, Pittsburgh, PA). Heat-induced epitope retrieval was performed by heating slides in a BioCare Medical Decloaking Chamber at 98°C for 30 min in Target Retrieval buffer, pH 6.0 (Dako, Carpinteria, CA), followed by a 30-min cool-down period. Slides were placed in TBST buffer (Thermo Scientific, Kalamazoo, MI) prior to assay. Endogenous peroxidases were blocked by incubating slides for 5 min in 3% aqueous hydrogen peroxide. Endogenous avidin and biotin were blocked by using a biotin-blocking system (Dako, Carpinteria, CA) for 10 min each followed by 30 min of incubation in Background Sniper (BioCare Medical, Concord, CA). For detection of type I pneumocytes, primary Syrian hamster anti-podoplanin 38 antibodies (eBioscience, San Diego, CA), diluted 1:2,000, were applied for 1 h to lung sections. After rinsing, the secondary biotinylated rabbit anti-Syrian hamster antibodies (Abcam, Cambridge, MA) were applied to sections at 1:200 for 30 min. Detection of bound secondary antibodies was performed with horseradish peroxidase-labeled streptavidin (Thermo Scientific, Kalamazoo, MI), with 3,3′ diaminobenzidine (Thermo Shandon, Pittsburg, PA) for 5 min as a chromogenic substrate, and with a light hematoxylin counterstain (Thermo Scientific, Kalamazoo, MI). Grading and description of pathology were performed by an experienced veterinary pathologist (P. Vogel) in a single-blind manner with respect to the purpose of the study and the composition of the groups.

Lung viral and bacterial titers. The lungs were removed under sterile conditions, washed 3 times with PBS, homogenized, and suspended in PBS (total volume, 1 ml). The suspensions for virus titration were centrifuged at 2,000 × *g* for 10 min to clear cellular debris. Virus titers were determined by plaque assays in MDCK cells. Lung homogenates were used directly for bacterial cultures prior to centrifugation. Pneumococcal colony counts were done by using 10-fold dilutions on tryptic soy agar plates (Difco Laboratories, Detroit, MI) supplemented with 3% (vol/vol) sheep erythrocytes and 400 μg/ml kanamycin.

Analysis of morphologically changed cells and immune and cytokine responses in the BAL fluid. After mice were euthanized by CO_2 inhalation, the trachea was exposed and cannulated with a 24-gauge plastic catheter (Becton, Dickinson Infusion Therapy Systems, Inc., Sandy, UT). Lungs were subjected to lavage twice with 1.5 ml of cold, sterile Hank's buffered salt solution. Cells were separated from fluid by centrifugation at 6,000 × *g* for 10 min, and the BAL fluid was stored at −80°C until use. Erythrocytes were digested with cold ammonium chloride (red blood cell [RBC] lysis buffer, Sigma, St. Louis, MO), and the total number of white blood cells (WBCs) was counted on a Countess automated cell counter (Invitrogen/Life Technologies, Grand Island, NY). Cells were resuspended in PBS, cytospun (Thermo Scientific, Ashville, NC) onto glass slides, and differentially stained (Quik-Dip stain; Mercedes Medical, Sarasota, FL). Neutrophils, monocytes/macrophages, and lymphocytes were identified by morphology and counted in 5 randomly selected high-power fields (~ 200 cells each). The numbers of epithelial and mononuclear cells with fragmented nuclei and vacuolated cytoplasm were counted to quantify cell damage in the airways. Concentrations of total IgA (Bethyl Laboratories, Montgomery, TX), interleukin-6 (IL-6), tumor necrosis factor alpha (TNF-α), beta interferon (IFN-β), and IFN-γ (BD OptEIA, San Diego, CA) in the BAL fluid were determined by enzyme-linked immunosorbent assay (ELISA) according to manufacturer guidelines.

Statistical analyses. Comparisons of survival rates of groups of mice were done using the log rank chi-square test to analyze Kaplan-Meier survival data over the period of 21 days. The mean number of days until death was estimated as the number of days that the mice survived after peptide administration or viral or bacterial infection. If no death occurred during the observation period, the mean number of days to death was considered to be 21 days. Comparisons between two matched groups of mice were achieved using an unpaired two-tailed Student's *t* test, whereas multiple comparisons were done by analysis of variance (ANOVA) followed by Tukey's multiple-comparison test. A P value < 0.05 was considered significant for these comparisons. Statistical analyses were performed using GraphPad Prism Software version 4.00 (GraphPad Software Inc., San Diego, CA).

RESULTS

Cytotoxic effects of PR8 PB1-F2 map to amino acid residues I68, L69, and V70. Sequence analysis of PB1-F2 C-terminal ends (aa 61 to 87) of viruses causing high (PR8 and WSN; H1N1) or low (the pandemic strains 1918, 1957, and 1968; a recent highly pathogenic avian IAV of the H5N1 subtype; and recent seasonal H3N2 1995) levels of death (6, 20, 21) suggested that amino acids I68, L69, and V70, present only in PR8 and WSN PB1-F2 (Fig. 1), are likely to contribute to the high level of death caused by these viruses. To confirm this proposition, we synthesized the 27-mer PR8 PB1-F2-derived C-terminal peptide and rescued a virus variant with mutations I68T, L69Q, and V70G designed to knock out the activity of the identified sequence.

Examination of cytotoxicity caused by exposure to 100 μM PR8 PB1-F2-derived peptides showed the ability of the C-terminal (PR8/C) to induce death in about 80% of epithelial MDCK and A549 cells and in about 61% of human monocytic U937 cells (Fig. 2A). In contrast to PR8/C, a peptide with triple I68T, L69Q, and V70G mutations (PR8/C-3) prompted death in only 5% to 17% of cells. Single substitutions of I68T, L69Q, or V70G did not reduce the level of PR8/C peptide cytotoxicity (data not shown), suggesting that high peptide cytotoxicity is a result of the presence of at least two residues but not one specific residue. Our previously published data from flow cytometric analysis indicated that cells exposed to the PR8/C peptide were dying as a result of necrosis (followed by cell lysis) rather than apoptosis (6). The live image of MDCK cells exposed to 100 μM PR8/C confirmed this proposition (Fig. 2B). The vast majority of cells exposed to PR8/C were permeable to nucleic acid staining. However, no signs of apoptosis (such as cell blebbing, fragmentation, or formation of apoptotic bodies) were observed, suggesting the necrotic type of cell death. In addition, pretreatment of cells with antiapoptotic pan-caspase inhibitor Q-VD-OPh did not protect them from killing by PR8/C (data not shown).

To investigate the cytotoxic properties of the PR8 PB1-F2 I68, L69, and V70 motif in the background of another virus, we introduced T68I, Q69L, and G70V mutations into the Wuh95 PB1-F2-derived peptide, which had not previously elicited any pathogenic effects in *in vitro* and *in vivo* systems (6, 8). Similar to PR8/C, the Wuh95/C + 3 peptide (with the I68, L69, and V70 sequence) caused significantly higher levels of death than its wild-type counterpart in all tested cell monolayers (Fig. 2A and B; $P < 0.05$). This suggested that the presence of the I68, L69, and V70 motif may contribute to a cell death phenotype of PB1-F2 proteins from other influenza A viruses.

We next examined the uptake and intracellular distribution of PR8 PB1-F2-derived peptides in cells (Fig. 2C). Both the wild-type and mutant peptides were distributed throughout the total depth of the slices, suggesting cellular internalization. Predominant cytoplasmic localization was noted in both cases. These data suggest that the presence of the I68, L69, and V70 motif in PR8/C

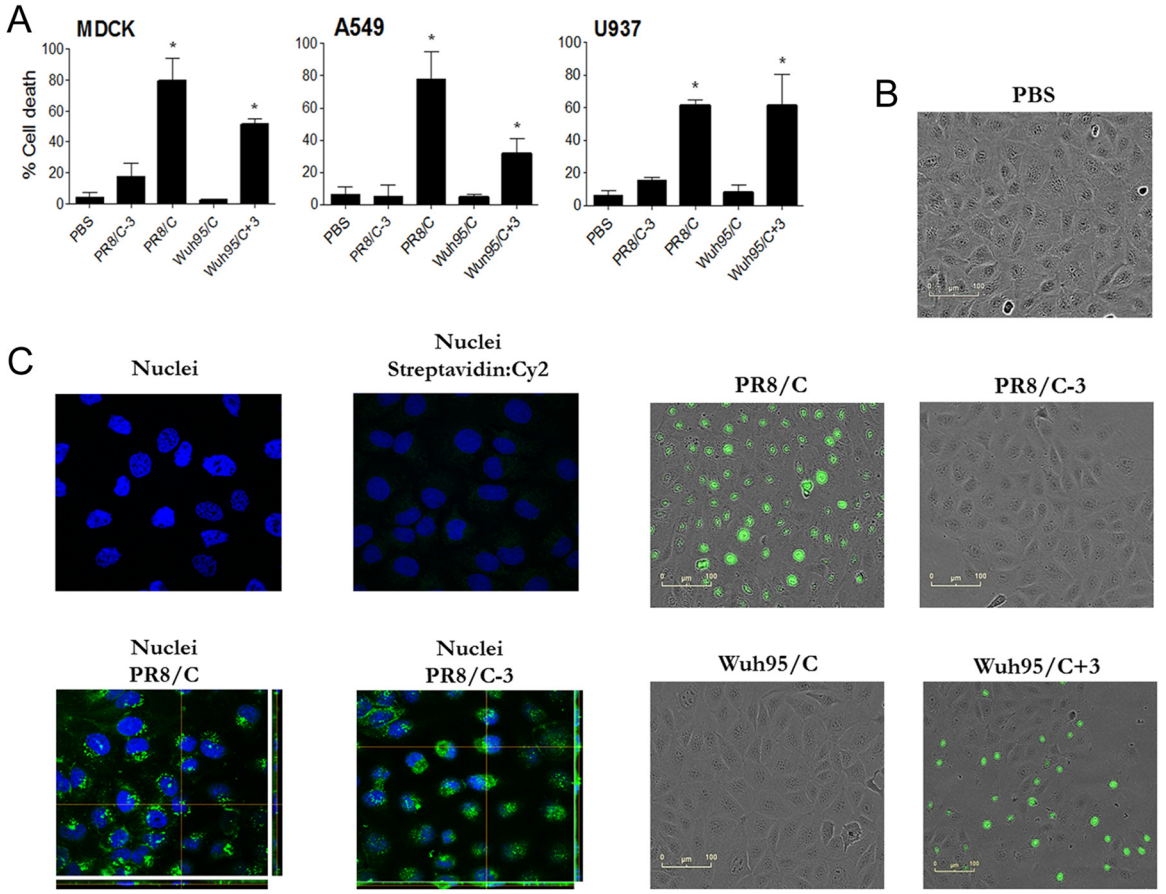

FIG 2 Amino acid sequence I68, L69, and V70 of PR8 PB1-F2 enhances death in various cell lines. (A) Exposure to 27-mer peptides derived from the C-terminal region of the PR8 or Wuh95 PB1-F2 proteins (see Fig. 1 for definition; final concentration for each peptide, 100 μM) or PBS for 1 h. The PR8/C and Wuh95/C + 3 PB1-F2-derived peptides contained the I68, L69, and V70 sequence. In Wuh95/C + 3, this sequence was introduced by mutations T68I, Q69L, and G70V. Wuh95/C and PR8/C-3 did not have the I68, L69, and V70 motif. In PR8/C-3, this motif was knocked out by mutations I68T, L69Q, and V70G. The proportions of live and dead cells in the samples were determined by exclusion of trypan blue. An asterisk indicates a significant ($P < 0.05$) difference by ANOVA compared with the results for the PBS or peptides without the I68, L69, and V70 sequence (PR8/C-3 and Wun95/C). (B) Image of live (unstained) and dead (stained with Sytox green nucleic acid stain) MDCK cells exposed to 80 μM PR8 or Wuh95 PB1-F2-derived peptides for 30 min. (C) Intracellular distribution of PR8 PB1-F2-derived peptides. Representative confocal Z-stack images of MDCK cells exposed to 50 μM (final concentration) PR8/C and PR8/C-3 biotinylated peptides for 1 h and stained with streptavidin:Cy2 are shown. Green staining represents PB1-F2-derived peptide, and blue represents nuclear staining.

contributes directly to cell death rather than indirectly through enhanced intracellular uptake.

To determine the potential of the PR8 PB1-F2 I68, L69, and V70 sequence to permeabilize mitochondrial membranes (similar to cell wall membranes), we exposed mitochondria isolated from the mouse liver to a 1,000 μM concentration of versions of PR8 PB1-F2 C-terminal peptide (with no, single, or triple I68T, L69Q, and V70G mutations; e.g., PR8/C-3) and analyzed the MOMP by the cytochrome *c* release into the supernatant. The PR8/C peptide promoted MOMP, while exposure of mitochondria to PR8/C-3 did not lead to cytochrome *c* release into the supernatant (Fig. 3). Similar to the data obtained in cytotoxicity assays, single mutations at any of these amino acid positions did not abolish the ability of PR8/C to promote cytochrome *c* release, suggesting that MOMP promotion is a combined effect of at least two residues but not one specific residue.

We next evaluated the role of the PB1-F2 I68, L69, and V70 sequence in the enhancement of cell death, the reduction of MTP, and the protein's mitochondrial localization in viral infection. Because these parameters depend on the virus level, we first examined the replication kinetics of PR8 and its virus counterpart containing I68T, L69Q, and V70G mutations in the PB1-F2 ORF (PR8-3) in various cell lines (Fig. 4). The results from growth kinetics experiments indicated that the effect of the PB1-F2 I68, L69, and V70 sequence on PR8 replication in tissue culture cells is negligible.

Flow cytometric analysis of apoptotic (annexin V^+ and PI^-) and necrotic (annexin V^+ and PI^+) events and MTP in U937 cells (shown to promote PB1-F2-induced apoptosis [3, 10]) infected with PR8 and PR8-3 at MOI = 3.0 did not reveal significant differences in these parameters between the two viruses 12, 24, or 48 h p.i. (data not shown). Thus, at 12 h p.i., both PR8 and PR8-3 viruses increased the level of U937 death by 12% and reduced MTP by 15%. Consistent with these data, the confocal microscopy of MDCK cells infected with PR8 and PR8-3 did not reveal significant differences in cellular localization of PB1-F2 proteins from the two viruses 8 h p.i. (Fig. 5A and C). Thus, approximately 75% to 90% of PB1-F2 proteins from PR8 and PR8-3 localized to mi-

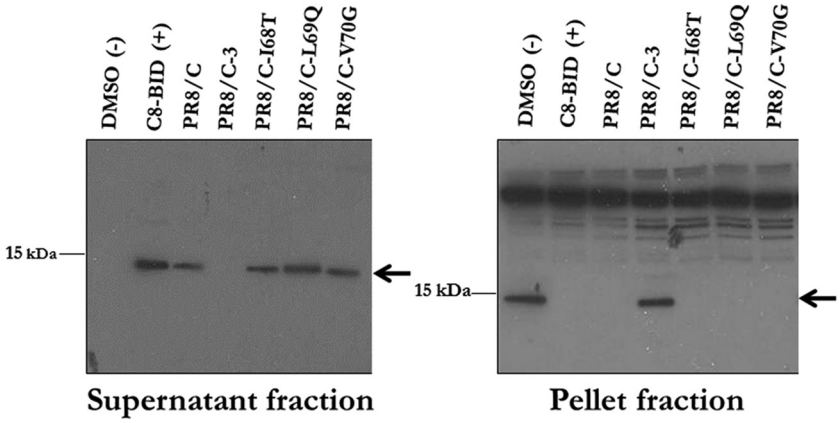

FIG 3 MOMP promotion by the I68, L69, and V70 sequence of PR8 PB1-F2. Western blot analysis of cytochrome *c* release into the supernatant after exposure of heavy membrane fractions (mitochondria) from mouse liver to 1,000 μM PR8/C (with the I68, L69, and V70 sequence) or PR8/C-3 (with I68T, L69Q, and V70G mutations) or PR8/C peptide with single substitutions at the desired residues for 45 min at 37°C was performed. The pellet fraction contains intact mitochondria with unreleased cytochrome *c*. C8-BID was used as a positive control for mammalian mitochondria. Arrows show cytochrome *c* in supernatant or pellet fractions.

tochondria. Interestingly, we observed approximately 60% less PB1-F2 protein expressed from PR8-3 than from PR8 8 h p.i. ($P < 0.05$; Fig. 5A and B).

The results of the experiments described here indicate that the newly identified I68, L69, and V70 amino acid sequence is responsible for the high level of death in the cell monolayers exposed to the PR8 PB1-F2/C peptide. This cytotoxic sequence of the PR8 PB1-F2/C peptide was shown to permeabilize cytoplasmic and isolated mitochondrial membranes. However, the differences in the levels of cell death between PR8 and a virus with the cytotoxic motif knocked out were negligible in *in vitro* cell systems.

The I68, L69, and V70 sequence of PB1-F2 increases PR8 pathogenicity in mice. To investigate whether cytotoxic properties of the I68, L69, and V70 amino acid sequence contribute to PB1-F2 pathogenicity in *in vivo* systems, we administered PR8/C and PR8/C-3 peptides a single time to groups of BALB/c mice ($n = 10$) i.n. at dosages ranging from 5 to 60 mg per mouse, or we infected mice i.n. with 15 PFU of PR8 or PR8-3. The differences in pathogenicity between the two peptides were evaluated by measuring weight loss and mortality, and the differences between the two viruses were evaluated by measuring virus lung titers. The inflammatory responses in mice were examined in both peptide and virus cases.

Exposure of mice to high dosages such as 30 or 60 mg PR8 PB1-F2-derived peptides did not reveal significant differences in mortality and weight loss between PR8/C (containing the cyto-

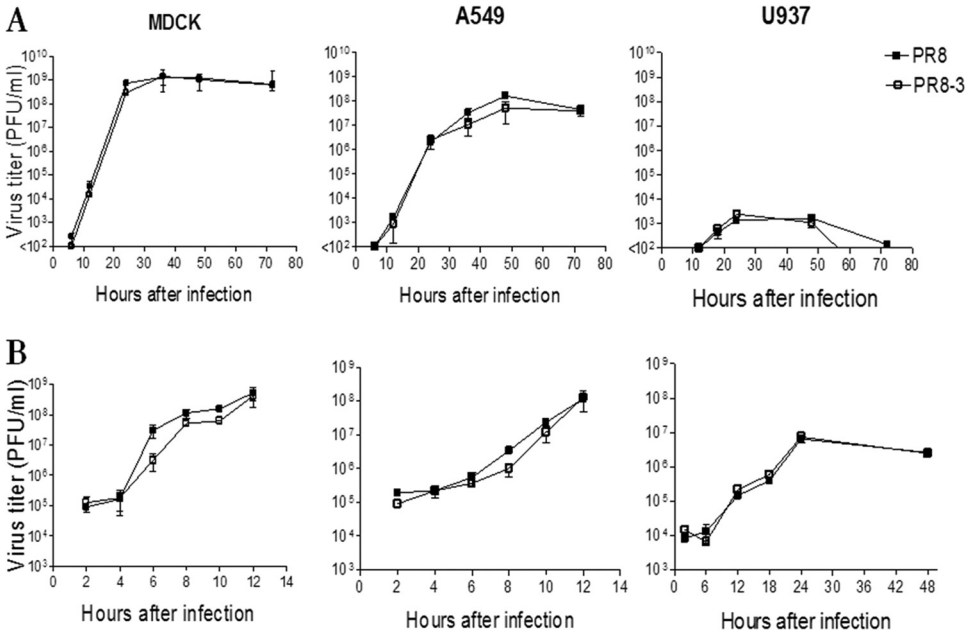

FIG 4 Growth kinetics of PR8 and PR8-3 in various cell lines. MDCK, A549, or U937 cells were infected with PR8 or an isogenic mutant altered at I68T, L69Q, and V70G of the PB1-F2 of PR8 (PR8-3) at MOI = 0.01 (A) or 3.0 (B). Virus titers were determined for culture supernatant fluids at the times indicated on the *x* axis. Error bars indicate the standard deviations (SD) of the means of the results from three independent experiments.

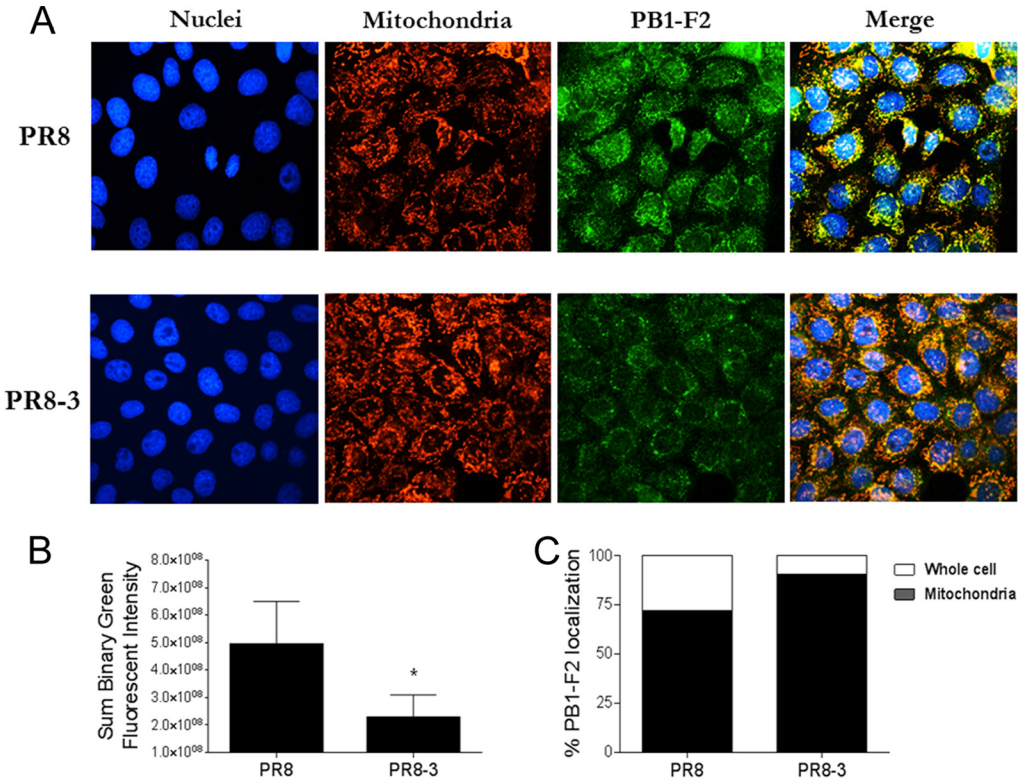

FIG 5 Expression and distribution of PB1-F2 proteins from PR8 and PR8-3. MDCK cell monolayers were infected with PR8 or PR8-3 virus at MOI = 3.0 for 8 h. The PR8-3 had I68T, L69Q, and V70G mutations in the PB1-F2 amino acid sequence. (A) Using confocal microscopy and antibodies specific for viral PB1-F2 or cell mitochondria, the sum binary fluorescent intensities were determined for five fields containing ~1,000 cells total. Cell nuclei were visualized with DAPI. Differences in PB1-F2 protein expression (green fluorescent signal) between PR8 and PR8-3 are visually notable in representative fields for each virus. Localization of PB1-F2 to mitochondria is indicated by the yellow color in the merged pictures. (B) Total fluorescent intensities from PB1-F2 proteins from PR8 and PR8-3 are expressed as means ± SD. An asterisk indicates a significant difference ($P < 0.05$) by ANOVA compared with the PR8 virus. (C) Predominant mitochondrial localization of PB1-F2 proteins from PR8 and PR8-3.

toxic sequence) and its triple-mutant variant PR8/C-3 (Table 1). Thus, all mice died after treatment with 60 mg of either peptide, and 70% to 80% of the mice died after treatment with 30 mg. Administration of the lower peptide dosage of 15 mg to mice (which caused 20% to 30% mortality in both groups) revealed significantly more weight loss in animals exposed to PR8/C than in those exposed to PR8/C-3 (25% weight loss versus 11% weight loss by 3 days after peptide exposure, respectively; $P < 0.05$; Fig. 6A).

TABLE 1 Survival of mice exposed to PB1-F2-derived peptides[a]

Peptides with I68, L69, and V70 amino acid sequence

Dosage (mg/mouse)	PR8/C			Wuh95/C + 3		
	Mean no. of days to death ± SD	Survival (%)	No. of survivors/total no. of mice	No. of survivors/total no. of mice	Survival (%)	Mean no. of days to death ± SD
5	>21	100	10/10	10/10	100	>21
15	15.0 ± 9.7	70	7/10	7/10[b]	70	15.0 ± 9.7
30	5.2 ± 8.4	20	2/10	1/10[b]	10	3.0 ± 6.3
60	1.0 ± 0.0	0	0/10	0/10[b]	0	1.0 ± 0.0

Peptides without I68, L69, and V70 amino acid sequence

Dosage (mg/mouse)	PR8/C-3			Wuh95/C		
	Mean no. of days to death ± SD	Survival (%)	No. of survivors/total no. of mice	No. of survivors/total no. of mice	Survival (%)	Mean no. of days to death ± SD
5	>21	100	10/10	10/10	100	>21
15	17.0 ± 8.4	80	8/10	10/10	100	>21
30	7.3 ± 9.5	30	3/10	10/10	100	>21
60	1.0 ± 0.0	0	0/10	10/10	100	>21

[a] BALB/c mice intranasally exposed to various dosages of PB1-F2 peptides were monitored for 21 days to determine the number of mice that died and the mean number of days to death. Control mice were treated with PBS alone (data not shown).
[b] The number of mice that survived exposure to peptide with mutations differed significantly from the number that survived exposure to the naturally occurring peptide, as compared by the Kaplan-Meier method followed by a log rank test.

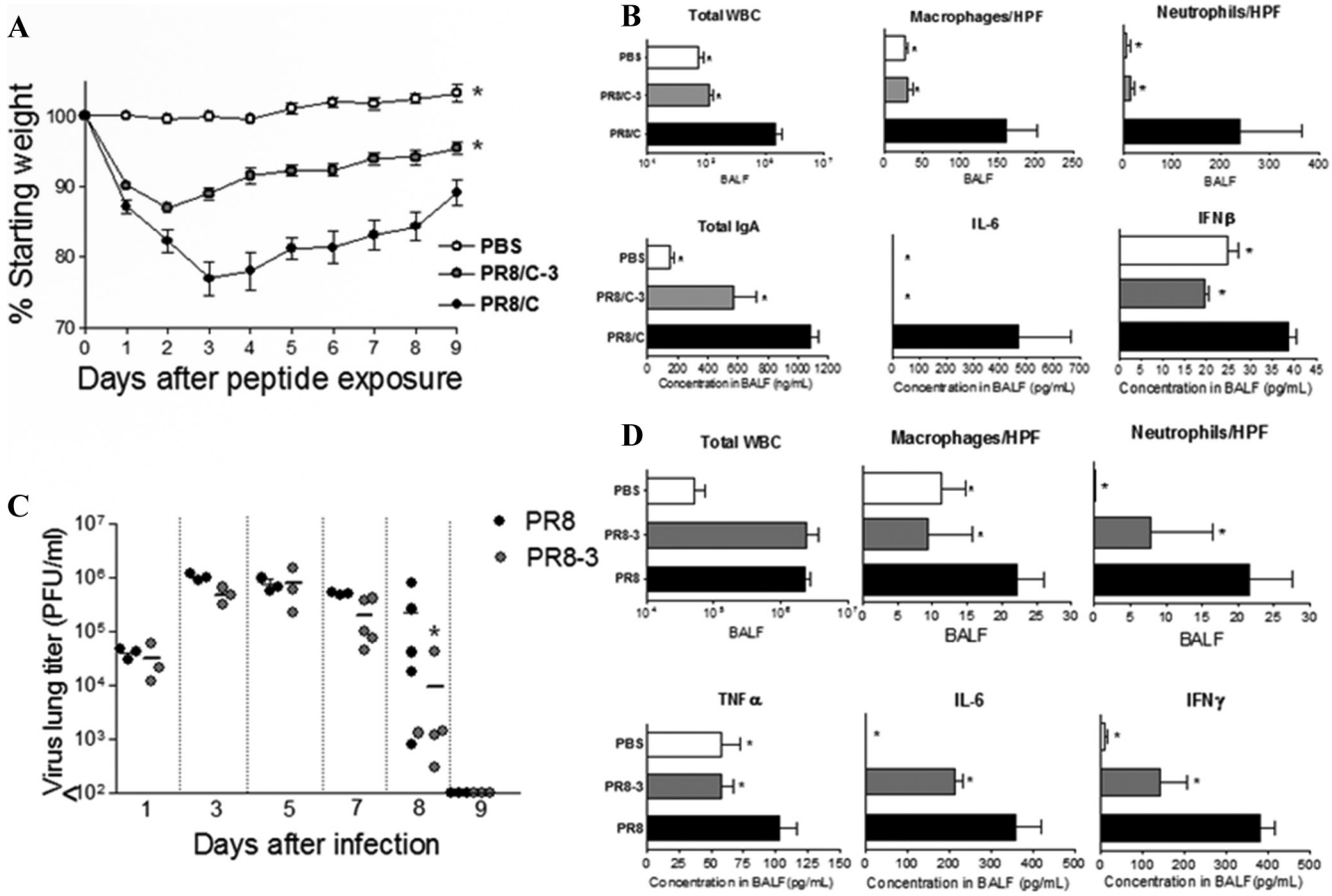

FIG 6 The I68, L69, and V70 sequence of PR8 PB1-F2 increases peptide and virus pathogenicity in mice. (A and B) Weight loss (A) and inflammatory and cytokine responses (B) in BALB/c mice exposed to 15 mg PR8/C- or C-3-derived peptides or PBS (as a control) 3 days after exposure. HPF, high-power field. (C and D) Virus lung titers (C) and inflammatory and cytokine responses (D) in mice infected with 15 PFU per mouse of PR8 and PR8-3. PR8/C-3 peptide and PR8-3 virus had I68T, L69Q, and V70G alterations in the PB1-F2 amino acid sequence. (A) Mice ($n = 10$) were monitored individually for weight loss; results are presented as mean percentages of starting weight ± SD. (B and D) Total white blood cells (WBCs), neutrophils, macrophages, IgA, and cytokines recovered from bronchoalveolar lavage (BAL) fluid of mice ($n = 5$) 3 days after peptide exposure (B) or 7 days after viral infection (D). Means ± SD are shown. (C) Growth kinetics of PR8 and PR8-3 viruses in lungs of mice ($n = 3$ to 5 per time point). An asterisk indicates a significant difference ($P < 0.05$) by ANOVA (A, B, and D) or by Student's *t* test (C) compared with the results for the mice exposed to the PR8/C peptide (A and B) or infected with the PR8 virus (C and D).

Single amino acid substitutions (I68T, L69Q, or V70G) did not influence the ability of the PR8/C peptide to induce weight loss (data not shown). In similarity to the PR8/C results, the presence of the I68, L69, and V70 sequence significantly ($P < 0.05$) enhanced the pathogenicity of the Wuh95/C + 3 peptide in mice (as measured by mortality) over that of naturally occurring peptide (Table 1).

Assessment of inflammatory cell responses and mucosal immunity and cytokines in the BAL fluid of mice exposed to PR8 PB1-F2-derived peptides showed significantly higher ($P < 0.05$) levels of total WBCs, macrophages, neutrophils, and IgA, along with cytokines, including IL-6 and IFN-β, in mice exposed to the PR8/C peptide than in mice exposed to PR8/C-3 or PBS (Fig. 6B).

In the virus context, the I68, L69, and V70 sequence of PB1-F2 supported PR8 replication in mice 8 days p.i. (Fig. 6C). During early infection time points (up to 7 days p.i.), we observed no significant differences in virus titers. After 8 days p.i., the differences in the mean viral titers became significant ($P < 0.05$) at mean levels of 9.0×10^3 PFU/ml for PR8-3 and 2.0×10^5 PFU/ml for PR8. Despite those differences, both viruses were cleared from the mouse lungs by 9 days p.i. Similar to the PB1-F2/C peptide, the PR8 with the I68, L69, and V70 sequence on its PB1-F2 elicited higher levels of inflammatory responses in mice (compared with the PR8-3 PB1-F2 mutant), as reflected by the levels of macrophages, neutrophils, and cytokines, including IL-6, TNF-α, and IFN-γ, in the BAL fluid 7 days p.i. ($P < 0.05$; Fig. 6D). Our findings indicated the ability of the I68, L69, and V70 sequence of PR8 PB1-F2 to enhance lung inflammation. Interestingly, the inflammation enhancement by the I68, L69, and V70 sequence seemed to be independent of the viral loads because the levels of PR8 and PR8-3 titers did not differ at this particular time.

Assessment of death in cells from BAL fluid cytospins 7 days p.i. by morphological analysis showed significantly more ($P < 0.05$) morphologically transformed epithelial and immune mononuclear cells recruited in the airways of PR8-infected mice than in the PR8-3 mutant group (Fig. 7B). The dislodged ciliated airway epithelial and mononuclear cells from BAL fluid of mice given PBS retained their round-oval nuclei, evenly stained cytoplasm, and cilia (for epithelial cells) (Fig. 7A). Cytospun BAL fluid of mice infected with PR8 (whose PB1-F2 has the I68, L69, and V70

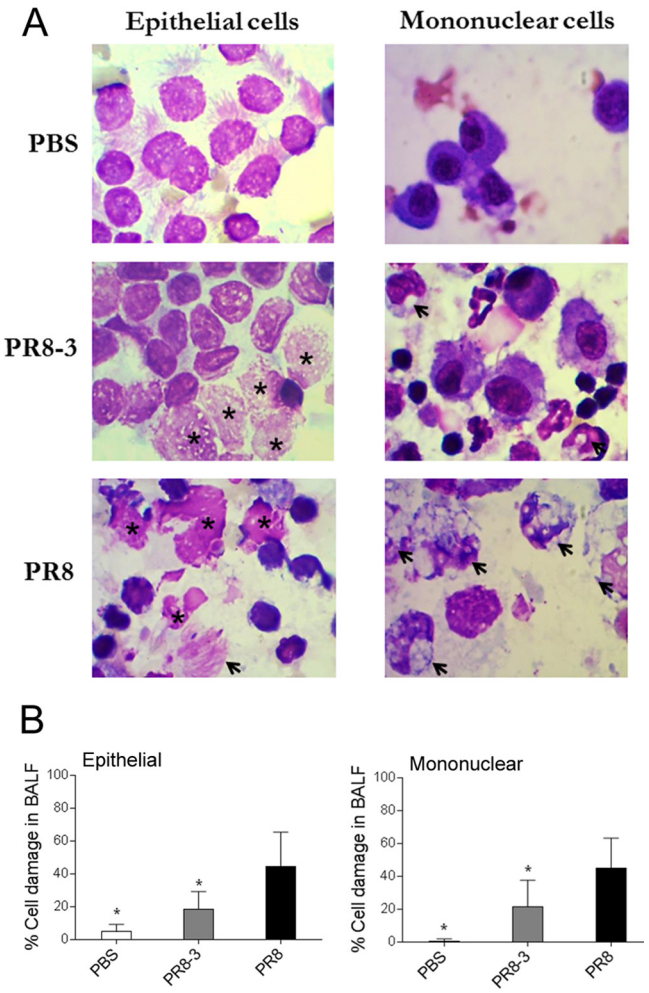

FIG 7 The I68, L69, and V70 sequence of PR8 PB1-F2 induces morphological changes in epithelial and mononuclear cells. Groups of mice were infected with 15 PFU per mouse of PR8 and PR8-3 (whose PB1-F2 had I68T, L69Q, and V70G amino acid alterations) or PBS (as a control) and euthanized 7 days after viral infection. Bronchoalveolar lavage fluid (BALF) of mice ($n = 5$) was harvested and separated from cells by centrifugation. (A) Epithelial or mononuclear cells from mice given PBS or infected with PR8-3 or PR8 were cytospun, differentially stained, and counted at ×1,000 magnification using light microscopy. Differentiation of morphologically altered (see definition in Materials and Methods) epithelial or mononuclear cells was done using standard morphometric techniques. An asterisk specifies fragmented nuclei; the arrow shows separated cilia or vacuoles in cytoplasm. (B) Cells (at least 1,000) in five random fields per sample were counted to estimate the percentages (means ± SD) of morphologically changed epithelial or mononuclear cells. Asterisks indicate a significant ($P < 0.05$) difference by ANOVA compared with the results for the PR8-infected group.

sequence) contained numerous epithelial cells with fragmented nuclei and separated cilia. Mononuclear cells in these samples also showed distinctive morphological features of death, such as fragmented nuclei and highly vacuolated cytoplasm. In contrast to infection with PR8, infection of mice with the PR8-3 mutant resulted in few epithelial cells containing fragmented nuclei and mononuclear cells displaying morphological signs of damage.

The data from experiments described here indicate that the I68, L69, and V70 sequence can elevate PR8 PB1-F2-mediated morbidity by increasing the mouse weight loss caused by peptide administration, lung titers and damaged epithelial and immune cells caused by viral infection, and mouse host immune responses in both cases.

The I68, L69, and V70 sequence of PR8 PB1-F2 primes for bacterial pneumonia in mice. To determine whether the enhanced pathogenicity of PR8 PB1-F2 with the I68, L69, and V70 motif accelerates the development of secondary bacterial pneumonia in mice, we treated mice with a nonlethal dose of 10 mg per mouse of PR8/C or C-3 peptides or PBS and 1 day later challenged them with 2,000 CFU of SPn. Weight loss and survival of mice dosed with peptides were monitored for 21 days after the bacterial challenge. In the case of viral infection, we infected mice ($n = 10$) with a nonlethal dose of 15 PFU of PR8 or PR8-3 (with I68T, L69Q, and V70G mutations in the PB1-F2) per mouse and 7 days later challenged them with a nonlethal dose of 100 CFU of SPn per mouse. The differences in pathogenicity between the two viruses were evaluated by measuring the viral and bacterial lung titers and survival.

Mice exposed to either PB1-F2-derived peptide showed comparable levels of weight loss (11.6% for PR8/C and 8.6% for PR8/C-3) by the time (day 0) of bacterial infection (Fig. 8A). Subsequent challenge with SPn enhanced this weight loss (to 23.3% by 3 days p.i.) and had a significant effect on mortality (60% by 11 days p.i.; $P < 0.05$; Fig. 8B) only in the group of mice exposed to PR8/C with the I68, L69, and V70 sequence. The level of mortality in the group of mice given PR8/C-3 was similar to that of mice given PBS and subsequently infected with SPn. Examination of mouse lung bacterial titers showed that the excessive weight loss and mortality observed in the mice exposed to the PR8/C peptide were due to mean bacterial lung titers as much as 20 times those in the mice given the mutant peptide (Fig. 8C). Of note, 6 of 10 mice in the group given PR8/C-3 had cleared bacteria from the lungs by that time. Bacterial growth was not observed in the lungs of mice given PBS. Quantification of the immune cells in BAL fluid indicated significantly higher levels of total WBCs, neutrophils, and lymphocytes in mice exposed to the PR8/C peptide than in those given PR8/C-3 or PBS ($P < 0.05$; Fig. 8D).

Examination of the lungs for histopathologic changes in a bacterial pneumonia model revealed much more extensive and severe multifocal inflammatory lesions in the lungs of mice given the PR8/C peptide (overall severity of 31.2 ± 6.3 by semiquantitative scoring) than in those given the peptide lacking the I68, L69, and V70 motif (overall severity score of 8.3 ± 4.5; Fig. 9, upper panel). The inflammatory lesions in the lungs of mice exposed to PR8/C were characterized by extensive areas of alveolar collapse and infiltration by mixed inflammatory cells and filling of affected alveoli with neutrophils and cell debris. In affected areas, there was frequently loss or attenuation of terminal bronchiolar epithelium. In mice given PR8/C-3, the inflammatory foci were generally limited to areas surrounding terminal airways and were characterized by mild to moderate interstitial and alveolar infiltrates of inflammatory cells that filled individual alveoli only rarely. There were no signs of lung inflammation in the control group that received PBS.

To determine whether the loss of the alveolar epithelium integrity contributed to the extensive lung damage caused by PR8/C, we stained sections of mouse lungs for podoplanin. Podoplanin, or type I cell α protein, is abundant in the apical membrane of the alveolar epithelial type I cells of rodent and human lungs (28) and is used as a marker of lung injury associated with functional damage to the alveolar epithelium (29, 30). Examination of the lungs

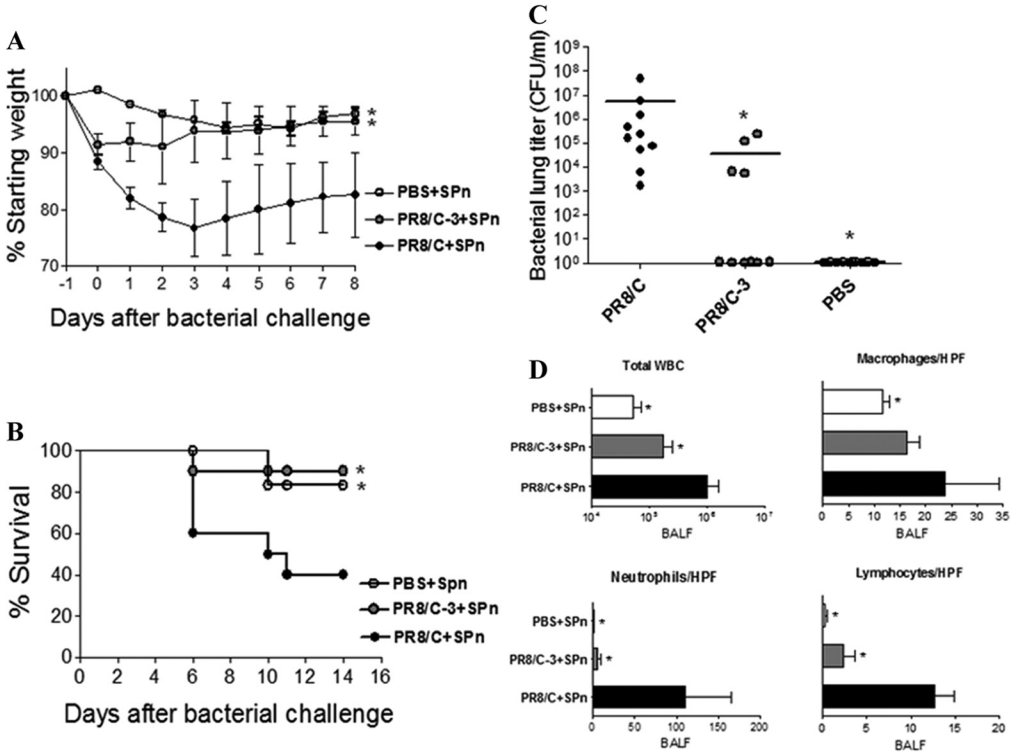

FIG 8 The I68, L69, and V70 sequence of PR8 PB1-F2 peptide accelerates bacterial pneumonia in mice. (A to D) Weight loss (A), survival (B), bacterial lung titers (C), and inflammatory cell recruitment (D) in mice exposed to PR8 PB1-F2-derived peptides. BALB/c mice ($n = 10$ each for panels A, B, and C) were exposed to 10 mg PR8/C or PR8/C-3 peptides or PBS and then challenged 1 day later with a dose of 2,000 CFU of *S. pneumoniae* (SPn) per mouse. (C) Lungs were collected 1 day after the challenge and titrated for bacterial load. (D) Total white blood cells (WBCs), neutrophils, macrophages, and lymphocytes recovered from the BAL fluid of mice ($n = 5$) 3 days after bacterial challenge. (A and D) Error bars indicate the SD of the mean. Asterisks indicate a significant difference ($P < 0.05$) compared with the PR8/C + SPn group by ANOVA (A and D), by Student's *t* test (C), and by the log-rank test on the Kaplan Meier survival data (B).

of mice exposed to either PR8/C or PR8/C-3 showed that changes in the extent and intensity of immunohistochemical staining for podoplanin were closely associated with the severity of pulmonary damage (Fig. 9; lower panel). Thus, podoplanin staining was markedly reduced or lost in affected areas of lungs of mice exposed to PR8/C and then SPn. This loss appeared to directly correlate with the severity of inflammation and alveolar collapse. In contrast, the reduced podoplanin staining in lungs exposed to PR8/C-3 typically appeared as incomplete coverage of alveoli with thickened septa and was generally limited to peribronchiolar alveoli. Podoplanin staining in lungs of mice exposed to PBS and SPn revealed complete coverage of alveoli by type I pneumocytes in normal lungs.

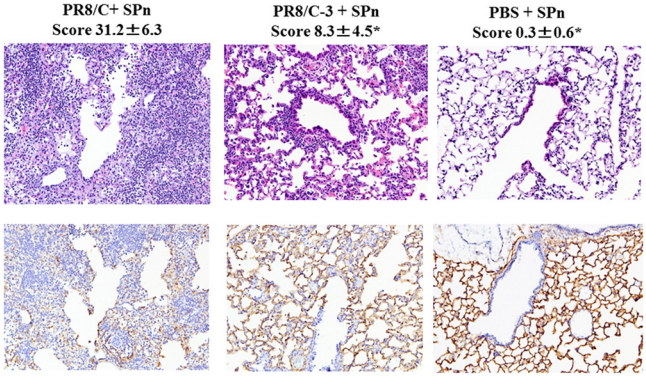

FIG 9 Histopathologic changes in the lungs of mice exposed to PR8 PB1-F2-derived peptides in a bacterial pneumonia model. Mice exposed to 10 mg PR8/C or PR8/C-3 (a version of PR8/C altered at I68T, L69Q, and V70G) peptides or PBS were challenged 1 day later with a dose of 2,000 CFU of *S. pneumoniae* (SPn) per mouse. Sections of lungs stained with hematoxylin and eosin (upper panel) or podoplanin (lower panel [brown staining]) are pictured at ×20 magnification. A semiquantitative grading system was used to assess the degree of injury in each set of lungs. The total scores for all pulmonary lesions (means ± SD) determined for 3 mice per group are shown. Asterisks indicate a significant ($P < 0.05$) difference by ANOVA compared with the results for the PR8/C + SPn group.

Similar to the results seen with PR8 PB1-F2-derived peptides in the bacterial pneumonia model, infection of mice with PR8 promoted development of secondary bacterial infection to a significantly greater extent than infection with its mutant virus counterpart, as determined by the levels of synergistic viral and bacterial titers and survival. Thus, for the group of mice infected with PR8 and 7 days later challenged with SPn, the mean levels of virus lung titers were 20- to 40-fold higher than those in mice infected with PR8-3 2 days and 1 day after bacterial challenge, respectively (Fig. 10A). Both viruses were cleared from the mouse lungs by 3 days after bacterial challenge. The mean levels of bacterial lung titers were also significantly higher (25- to 70-fold 1 and 3 days after bacterial challenge, respectively) in the mice infected with PR8 than in those infected with the PR8-3 mutant ($P < 0.05$; Fig. 10B). The differences in the mean bacterial lung titers between the two viruses were not so distinct 2 days after bacterial challenge. However, 5 of 10 mice infected with the PR8-3 mutant but none infected with PR8 had cleared the bacteria from their lungs by that

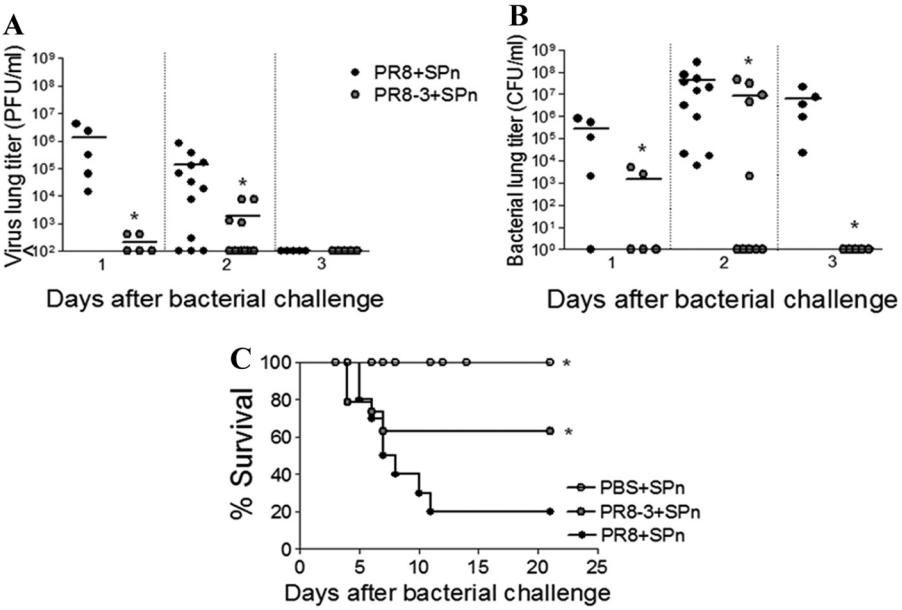

FIG 10 Secondary bacterial pneumonia in PR8- or PR8-3-infected mice. BALB/c mice were infected with a sublethal dose of 15 PFU per mouse of PR8, PR8-3, or PBS and then challenged 7 days later with a sublethal dose of 100 CFU of *S. pneumoniae* (SPn) per mouse. (A and B) Lungs from 5 to 12 mice were collected 1, 2, and 3 days after bacterial challenge and titrated for viral and bacterial load. (C) Survival of a group of mice ($n = 10$) was monitored for 21 days after bacterial challenge. Asterisks indicate a significant ($P < 0.05$) difference compared with the PR8-infected group by Student's *t* test (A and B) and the log-rank test performed on the Kaplan Meier survival data (C).

time. Higher mean bacterial and viral lung titers resulted in a significantly lower survival rate for mice infected with PR8 than for those infected with PR8-3 in a secondary bacterial infection model (20% survival versus 60% survival, respectively; $P < 0.05$; Fig. 10C).

DISCUSSION

The experiments with PB1-F2-derived peptides and their virus counterparts presented here indicate that the presence of the I68, L69, and V70 sequence on PR8 PB1-F2 significantly accelerates the development of pneumococcal infection and associated mortality.

The role of virus-induced death in the host-pathogen interaction is not clear. The IAV protein PB1-F2 was shown to induce cell death related to mitochondrial targeting (3, 10, 14) or formation of β-amyloid pore structures (24) in *in vitro* systems and to activate genes linked to cell death (along with genes linked to inflammatory response and neutrophil chemotaxis) in *in vivo* models (21). The enhancement of cell death by PB1-F2, however, seems be restricted to only some IAVs. Among tested PB1-F2 proteins originating from several human H1N1 and H3N2 strains and from highly pathogenic avian H5N1, only the PB1-F2 from H1N1 laboratory-adapted strain PR8 was shown to induce a high level of cell death (6). Based on the data from that prior work and recent publications showing PB1-F2-associated death with WSN influenza virus (20, 21), we charted the I68, L69, and V70 amino acid sequence within PB1-F2 (Fig. 1) and gained insights into its role in the cell death enhancement and pathogenicity of primary viral and secondary bacterial infections.

We determined that the presence of I68, L69, and V70 residues on the PR8 PB1-F2-derived peptide enhanced its cytotoxicity in cell cultures (causing necrotic death), its ability to permeabilize membranes in isolated mitochondria, and its virulence in mice. In addition, introduction of this sequence into the nonpathogenic H3N2 Wuh95 peptide converted it to a cytotoxic version. Consistent with the data on the peptides, infection of mice with PR8 significantly elevated the number of dying epithelial and immune cells in cytospun BAL fluid over that seen with infection with the PR8-3 mutant (without the I68, L69, and V70 motif). Residues 68 to 72 of PR8 PB1-F2 were recently identified as a region with a high propensity for aggregation (31). Such an "aggregation-prone" region may play a major role in determining PR8 PB1-F2's tendency to form amyloid fibrils and, associated with them, toxic effects (24). Introduction of I68T, L69Q, and V70G mutations could possibly reduce the ability of PB1-F2 to form amyloid fibrils, thus lessening cell toxicity (as observed with the PR8/C-3 peptide and PR8-3 mutant). However, we did not detect differences in the levels of cell death between PR8 and its PB1-F2 mutant virus variant in cell cultures. We do not know the exact factors contributing to this *in vitro* result. It is possible that the level of PR8 PB1-F2 expression in cell cultures (like the dose of intracellular PR8/C peptide or the level of PB1-F2 produced during viral infection *in vivo*) is not high enough to elicit noticeable cytotoxic effects. Interestingly, we detected a significantly lower level of PB1-F2 mutant expression from PR8-3 than from the wild-type virus in *in vitro* systems. However, the reduced PR8-3 PB1-F2 expression did not change the virus phenotype in cell cultures. Similar to our findings, the effect of low expression was observed with the N66S mutant form of PB1-F2 from the A/Viet Nam/1203/2004, VN1203 (H5N1), virus (32), suggesting the possibility of specific proteasomal degradation of the PB1-F2 mutant variants. However, this proposition needs to be confirmed.

Administration of the C-terminal PB1-F2-derived peptide of PR8 (with the I68, L69, and V70 motif) to mice elicited elevated inflammatory responses (as reflected by the levels of total WBCs, macrophages, neutrophils, and proinflammatory cytokines in the

BAL fluid), resulting in increased weight loss. Similar to the peptide, infection of mice with PR8 significantly enhanced inflammatory responses (compared with those of a virus without the cytotoxic sequence on its PB1-F2; i.e., PR8-3). Our findings suggest that the PR8 PB1-F2 protein increases lung inflammation, which can be a combined result of several factors. One of them might be increased damage to phagocytic cells in BAL fluid of mice by the cytotoxic sequence (I68, L69, and V70) of PR8 PB1-F2. This injury to macrophages or adjacent epithelial cells may increase the potential for infected cells to undergo primary or secondary necrosis, resulting in extensive tissue damage and a release of proinflammatory stimuli.

The phenomenon of lung inflammation accelerated by the cytotoxic sequence of the PR8 PB1-F2 protein has been indirectly confirmed by a recent study that used the PB1-F2 protein (also with the I68, L69, and V70 amino acid sequence) from WSN, another virus causing a high level of death (21). IFN-γ was identified as one of the central regulators of the PB1-F2-regulated inflammatory genes. It was proposed that PB1-F2-induced exacerbation of IFN-γ expression contributes to the promotion of secondary bacterial pneumonia. In our study, the significant increase in the level of IFN-γ in the BAL fluid of mice infected with PR8 (versus the PR8-3 mutant), along with elevation of other inflammatory responses, was accompanied by significant promotion of secondary bacterial pneumonia with the PB1-F2 protein. The loss of type I pneumocytes contributed to the extensive lung damage observed in a bacterial pneumonia model with the PR8/C peptide. Although we do not have the ultrastructural findings needed to confirm that the loss of podoplanin in the lungs was actually due to the loss of type I cells rather than to downregulation of podoplanin, the incomplete podoplanin coverage of alveoli plus the leakage of fibrin into the alveoli after exposure to the PR8/C peptide strongly suggests damage to the alveolar lining caused by the I68, L69, and V70 motif in a bacterial pneumonia model. Interestingly, the differences between the abilities of two peptides (with or without the I68, L69, and V70 motif) to induce alveolar epithelium damage were not noted in mice exposed to peptides only. This suggests that a synergistic mode exists between the PB1-F2 cytotoxic sequence and the SPn disruption of type I pneumocytes.

Recently, the 68ILVF71 sequence of PR8 PB1-F2 was proposed to be associated with its continuous extensive C-terminal α-helix formation and relatively low protein pathogenicity (31). In the PB1-F2 proteins from pandemic H1N1 1918 and a recent avian IAV of the H5N1 subtype, this sequence was replaced by 68TP VS71 or 68TQGS71. Among these residues, the Thr, Gly, and Ser are known as helix breakers. Indeed, the PB1-F2 from these two viruses contains a loop region (aa 66 to 71) that divides the C terminus into two shorter helices. Such a divided C-terminal α-helix structure was proposed to enhance PB1-F2 pathogenicity. However, introduction of two (of the three) helix breaker residues (such as T68 and G68) into the PR8 PB1-F2 sequence did not increase but reduced the pathogenicity of both the peptide and the virus. This suggests that introduction of either Thr or Gly does not break the PR8 PB1-F2 C-terminal α-helix or that the primary amino acid sequence dominates over the secondary protein structure in determining PB1-F2 pathogenicity.

Analysis of the predicted amino acid sequences of PB1-F2 proteins from the Influenza Research Database (33) indicates that, in addition to the PR8 and WSN viruses, the I68, L69, and V70 motif is present in the PB1-F2 proteins of several other H1N1 IAVs that were circulating until 1956 (such as A/Fort Monmouth/1/47 and A/Beijing/11/56). Later, this sequence in the PB1-F2 of the H1N1 lineage was lost through truncation, probably as negative selection for a trait (inflammation) that was evolutionarily disadvantageous in mammalian lungs. The only two recent IAVs of the H1N1 subtype, A/Taiwan/3355/97 and A/Russia:St.Petersburg/8/06, have the original I68, L69, and V70 sequence on PB1-F2. Among IAVs of the H3N2 lineage, only the PB1-F2 from A/Victoria/68 has this sequence. In the context of our experimental data indicating the ability of the I68, L69, and V70 sequence of PB1-F2 to promote IAV pathogenicity and predisposition to secondary bacterial infection, we suggest that surveillance for this motif in clinical isolates expressing the full-length PB1-F2 protein would be beneficial.

In addition to the cytotoxic motif, the PB1-F2 protein of PR8 has amino acid residues L62, R75, R79, and L82, which enhance inflammation caused by the PB1-F2 protein from pandemic H3N2 A/Hong Kong/1/68 (8). The role of these PB1-F2 inflammatory residues in PR8 pathogenicity is not yet established. Our current data showing higher pathogenicity of PR8/C-3 than of Wuh95/C (Table 1), however, suggest that the C terminus of PR8 PB1-F2 has other amino acids (in addition to I68, L69, and V70) that contribute to its virulence. Interestingly, the other influenza virus with these two distinct (cytotoxic and inflammatory) PB1-F2 sequences, A/Taiwan/3355/97 (H1N1), was isolated from a patient with severe pneumonia (34). Further studies on the interaction of PR8 PB1-F2 protein cytotoxic and inflammatory sequences during primary viral and secondary bacterial infections may reveal new aspects of viral pathogenicity.

ACKNOWLEDGMENTS

This work was supported by the American Lebanese Syrian Associated Charities (ALSAC).

We acknowledge Victoria Frohlich and Jennifer Peters of the Cellular Imaging Shared Resource of St. Jude for assistance with confocal microscopy, Dana Lucas of the Flow Cytometry and Cell Sorting Shared Resource of St. Jude for assistance with flow cytometry analysis, Amy Iverson and Shane Gansebom for technical assistance, Stephan Ludwig and Jonathan Yewdell for provision of antibodies directed against PB1-F2, and David Galloway for editing the manuscript.

REFERENCES

1. **Wright PF, Neumann G, Kawaoka Y.** 2007. Orthomyxoviruses, p 1691–1740. *In* Knipe DM, Howley PM, Griffin DE, Lamb RA, Martin MA, Roizman B, Straus SE (ed), Fields virology, 5th ed. Lippincott Williams & Wilkins, Philadelphia, PA.
2. **McCullers JA, Huber VC.** 2012. Correlates of vaccine protection from influenza and its complications. Hum. Vaccin. Immunother. **8:**34–44. http://dx.doi.org/10.4161/hv.8.1.18214.
3. **Chen W, Calvo PA, Malide D, Gibbs J, Schubert U, Bacik I, Basta S, O'Neill R, Schickli J, Palese P, Henklein P, Bennink JR, Yewdell JW.** 2001. A novel influenza A virus mitochondrial protein that induces cell death. Nat. Med. **7:**1306–1312. http://dx.doi.org/10.1038/nm1201-1306.
4. **Conenello GM, Zamarin D, Perrone LA, Tumpey T, Palese P.** 2007. A single mutation in the PB1-F2 of H5N1 (HK/97) and 1918 influenza A viruses contributes to increased virulence. PLoS Pathog. **3:**e421. http://dx.doi.org/10.1371/journal.ppat.0030141.
5. **Conenello GM, Tisoncik JR, Rosenzweig E, Varga ZT, Palese P, Katze MG.** 2011. A single N66S mutation in the PB1-F2 protein of influenza A virus increases virulence by inhibiting the early interferon response in vivo. J. Virol. **85:**652–662. http://dx.doi.org/10.1128/JVI.01987-10.
6. **McAuley JL, Chipuk JE, Boyd KL, van de Velde N, Green DR, McCullers JA.** 2010. PB1-F2 proteins from H5N1 and 20th century pandemic